Research Report

95-50

Modeling of Motor Bearing Currents in PWM Inverter Drives

S. Chen, T.A. Lipo, *D. Fitzgerald

Wisconsin Power Electronics Center
University of Wisconsin-Madison
Madison WI 53706-1691

*MagneTek
16555 West Ryerson Road
New Berlin WI 53151

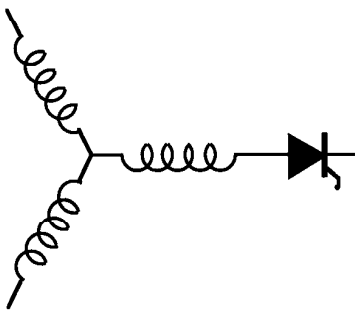

Wisconsin
Electric
Machines &
Power
Electronics
Consortium

University of Wisconsin-Madison
College of Engineering
Wisconsin Power Electronics Center
2559D Engineering Hall
1415 Johnson Drive
Madison WI 53706-1691

Modeling of Motor Bearing Currents in PWM Inverter Drives

Shaotang Chen Thomas A. Lipo Dennis Fitzgerald

Department of Electrical and Computer Engineering
University of Wisconsin-Madison
1415 Johnson Drive
Madison, WI 53706-1691 USA

MagneTek
16555 West Ryerson Road
New Berlin, WI 53151 USA

Abstract - *PWM inverters have recently been found to be a major cause of motor bearing failures in inverter-motor drive systems. Specifically, all inverters generate common mode voltages relative to the earth ground. The voltages provide coupling or bearing currents through motor parasitic capacitances to the rotor iron and then back from the bearings to the grounded stator case.*

In this paper, a model for bearing currents caused by PWM inverter is proposed. The model is based on transmission line theory which uses an equivalent lumped parameter π-network to describe the parasitic coupling phenomenon. The model parameters are then identified by matching the calculated model outputs with those of experimental measurement. The validation of the method is demonstrated by the fact that the model can reproduce all the experimental results obtained on a test motor.

An application of this method also gives a motor grounding current model. As the conducted EMI in drive systems is related to the grounding currents. The grounding current model can be used for the analysis of conducted EMI in motor-drive systems.

1. Introduction

Recently, PWM inverters have been found to be a major cause of motor bearing failures in inverter-motor drive systems. In principle, it has been found that all inverters generate common mode voltages relative to the earth ground which provide coupling and consequently bearing currents through the motor parasitic capacitances to the rotor iron then through the bearings to the grounded stator case [1, 2].

As is shown in Fig. 1, V_{AO} is the common mode voltage relative the negative DC bus, O, at motor phase A input terminal. Z_{in} is the common mode voltage internal impedance which usually consists of the parasitic coupling capacitance from negative DC bus to the earth. C_{ws} and C_{wr} are the coupling capacitances from motor windings to the stator and rotor iron respectively. C_g is the capacitance present across the bearings corresponding mainly to the motor air gap capacitance. The bearings are approximated by a switch B which turns on and off randomly due to motor rotating bearing electrical behavior. The bearing currents are the currents flowing into all C_{wr}'s and then back through switch B. Similarly, for phases B and C, common mode voltages V_{BO} and V_{CO} also contribute to the bearing current.

The distributed parameter circuit in Fig. 1 is, however, not suitable for a simplified analysis of the bearing currents. Equivalent lumped parameter circuit models are developed in this paper to describe the parasitic coupling phenomenon. In principle, the parasitic coupling circuits are the same as transmission line circuits. Based on transmission line theory, a distributed parameter circuit can be modeled by an equivalent lumped parameter π-network which gives the same input and output relationship. The method is applied to give a model of coupling from motor windings to stator irons - the motor grounding current model, and a model of coupling from motor windings to the rotor irons - the bearing current model. The model parameters are then identified by matching the calculated model outputs with those of experimental measurement. The validation of the model is demonstrated by the fact that the models can reproduce a variety of experimental results obtained on the test motor. Therefore, the proposed models can be used to analyze the effect of bearing currents and facilitate the determination of solutions to suppress these currents. As the motor grounding current is a major source of conducted EMI in inverter-motor systems, the motor grounding current model can thus be applied to the analysis of conducted EMI in motor-drive systems.

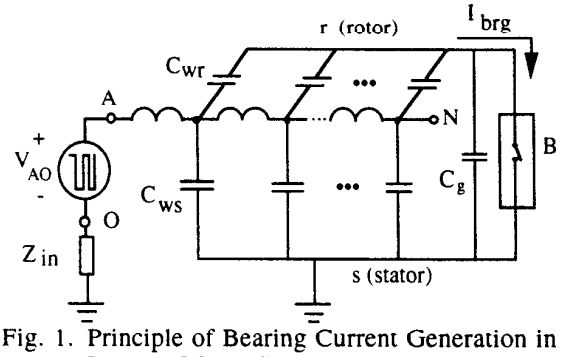

Fig. 1. Principle of Bearing Current Generation in Inverter-Motor System

2. Common Mode Excitation and Response

For a balanced three phase inverter-load system shown in Fig. 2, the three phase load is represented by Z. Assume that the zero sequence impedance of the load is Z_O and that there exists a common mode impedance Z_N from the neutral point to the ground. In such a system, both differential mode and common mode response exists. The purpose of this section is to derive a simplified common mode circuit model which describes only the common mode circuit response of the system.

In general, for a three-phase load Z, the zero sequence voltage and current are defined by

$$V_O = \frac{V_{AN}+V_{BN}+V_{CN}}{3} = \frac{V_A+V_B+V_C}{3} - V_N \qquad (1)$$

and

$$i_O = \frac{i_A+i_B+i_C}{3} \qquad (2)$$

respectively. The relationship between zero sequence voltage and current is governed by

$$V_O = i_O Z_O \qquad (3)$$

Based on the circuit, the common mode current and voltage at neutral point can be derived as

$$i_N = i_A+i_B+i_C = 3i_O = \frac{3}{Z_O+3Z_N}\frac{V_A+V_B+V_C}{3} \qquad (4)$$

and

$$V_N = \frac{3Z_N}{Z_O+3Z_N}\frac{V_A+V_B+V_C}{3} \qquad (5)$$

Since the common mode voltage V_N and common mode current i_N are the only physically meaningful common mode outputs in the system, it is seen that a model of common mode excitation can be obtained based on equations (4) and (5). By defining an equivalent common mode voltage input

$$V_{in} = \frac{V_A+V_B+V_C}{3} \qquad (6)$$

the common mode model can be simply represented by Fig. 3.

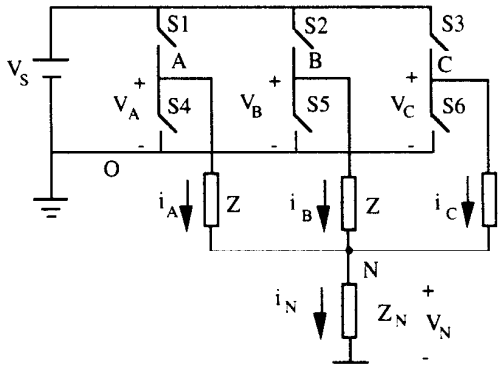

Fig. 2 Three-Phase Inverter-Load System Including Common Mode Impedance Z_n.

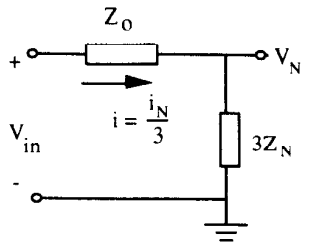

Fig. 3 Model of Common Mode Excitation

3. Modeling of Coupling from Windings to Stator - Motor Grounding Currents

As the coupling effect from the motor windings to the rotor iron is much smaller than that from the windings to stator laminations, it is first ignored in the following analysis. A distributed circuit model of coupling from the stator windings to the stator iron can be represented by Fig. 4. In Fig. 4, Z denotes the impedance per unit length of motor phase windings, and Z_{WS} the per unit length windings to stator parasitic coupling impedance which is mainly capacitive.

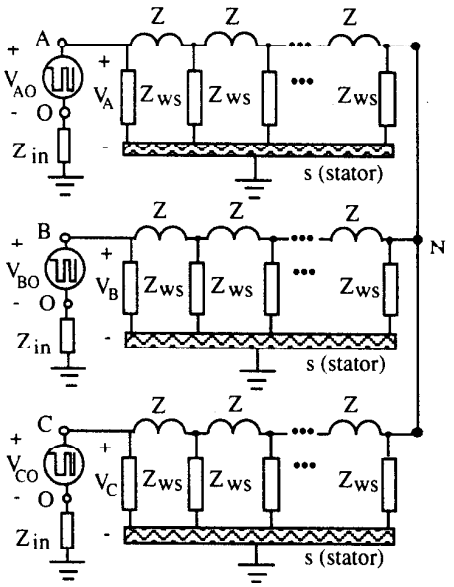

Fig. 4 Distributed Circuit Representation of Coupling from Motor Windings to Stator Laminations

Theoretically, the circuit represents a three-phase transmission line with one of its terminations shorted. As is treated in transmission line theory, if only the input and output characteristics are of interest, an equivalent π-network can be used to describe the input and output relationship. Thus, for each phase, the distributed parameter circuits can be replaced by an equivalent π-network. By

adding all three parallel connected neutral to ground impedances, an equivalent lumped parameter circuit model is obtain as shown in Fig. 5.. In this model, V_N is the voltage of motor neutral point and I_{WS} is the total coupling currents from windings to stator. All the parameters in the model are to be determined which are functions of Z and Z_{WS}.

Based on the derivation in Section 2, a simplified model of common mode excitation can be drawn as shown in Fig. 6 where L_O, C_O and R_O are the zero sequence components contained in L_S, C_S and R_S of Fig. 5. As the voltage of the motor neutral point and the total coupling currents from windings to stator are of interest, their relationship to the common mode input voltage V_{in} can be determined as

$$\frac{V_N}{V_{in}} = \frac{3Z_{WSN}}{Z_O + 3Z_{WSN}} \tag{7}$$

and

$$\frac{i_{ws}}{V_{in}} = \frac{3}{Z_{WS1}} + \frac{3}{Z_O + 3Z_{WSN}} \tag{8}$$

where Z_O, Z_{WS1} and Z_{WSN} are represented by (L_O, C_O, R_O), (L_{WS1}, C_{WS1}, R_{WS1}) and (L_{WSN}, C_{WSN}, R_{WSN}) respectively.

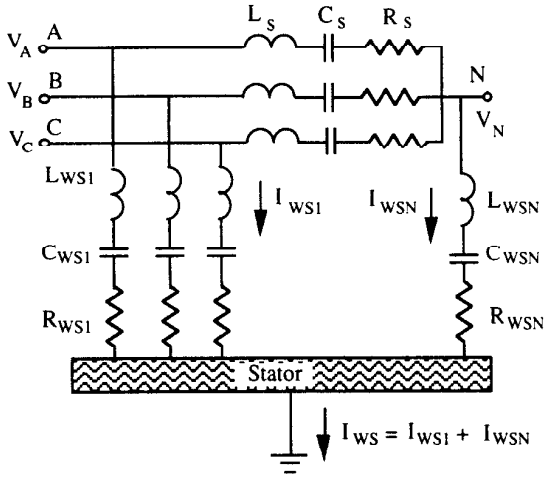

Fig. 5 An Equivalent Lumped Parameter Circuit Showing Coupling from Motor Windings to Stator Iron Laminations

It is obvious that the V_N is not related to impedance Z_{WS1}. For coupling currents, simulation based on the model shows that I_{WS1} is much larger than I_{WSN}. Therefore, the grounding current I_{WS} is primarily determined by Z_{WS1},while the motor winding neutral point voltage is governed by Z_{WSN}.

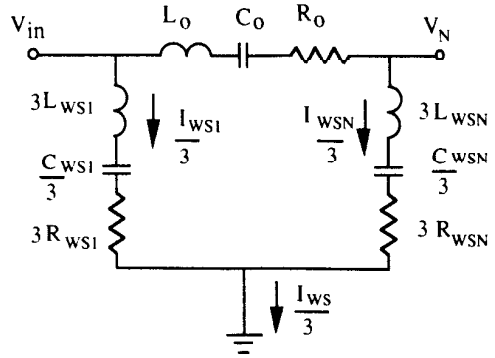

Fig. 6 Model of Common Mode Coupling from Windings to Stator Laminations

4. Modeling of Coupling from Windings to Rotor - Bearing Current Model

Bearing currents are only related to the common mode coupling from the windings to the rotor iron and are not represented in the circuit of Fig. 6. However, as both coupling currents to rotor and stator share the same path in the stator windings and the stator coupling currents are considerably large, the influence of stator coupling currents to the bearing current model should be taken into account.

In spite of above statement, let us first ignore for the moment the flow of stator coupling currents in the windings. Similar to Section 3, the same distributed parameter circuit of motor windings as shown in Fig. 4 can also be used to describe the coupling from windings to the rotor except that Z_{WS} has to be replaced by Z_{WR}. Also, in terms of input and output relationship, the rotor coupling circuit can be represented by an equivalent lumped π-network. A rotor coupling model together with an illustrated bearing block is depicted in Fig. 7.

Now, it is useful to consider the effect of stator coupling currents in the stator windings on the rotor currents. The equivalence of stator coupling is an impedance Z'_{WS1} connected from the input of each phase winding to the stator and an impedance Z'_{WSN} connected from the neutral point to the stator as shown in Fig. 5. It is apparent that Z'_{WS1} will have no influence on the bearing currents and voltages, while Z'_{WSN} represents those stator coupling currents which have an effect on the rotor coupling circuit. Therefore, the influence of stator coupling currents to the rotor coupling path can always be considered by adding an impedance L'_{WSN}, C'_{WSN} and R'_{WSN} to the circuit model as is indicated by the dashed line portion in Fig. 7. Notice that Z'_{WSN} and Z_{WSN} may not be the same.

The uncertainty of the exact value Z'_{WSN} clearly causes a small error in calculation of bearing

current i_{brg} and shaft voltage V_{brg} as has been observed in our simulation study. However, to simplify the analysis, we will neglect the influence of Z'_{WSN}. However, In case precise modeling of bearing currents is required, Z'_{WSN} can be readily added into the rotor coupling model as shown in Fig. 7.

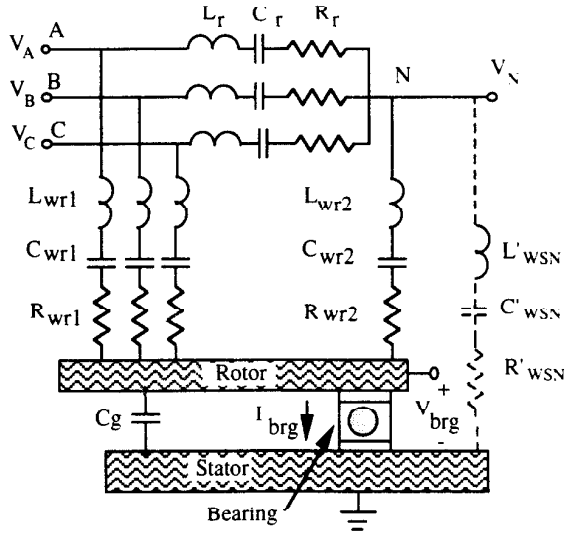

Fig. 7 Lumped Parameter Equivalent Circuit of Coupling from Stator Windings to Rotor Iron Laminations

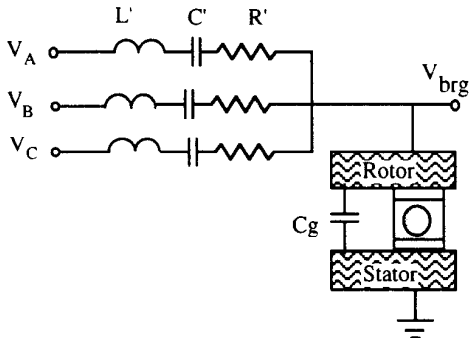

Fig. 8 Simplified Rotor Coupling Model Ignoring Influence of Stator Coupling Currents

By ignoring Z'_{WSN}, the circuit model shown in Fig. 7 can be simplified by replacing the π-network with a single L'C'R' component as shown in Fig. 8. The bearing model can then be combined with the coupling circuit which results in the circuit shown in Fig. 9. The bearings are modeled as a switch B with certain internal inductance L_B and resistance R_B.

Finally, as the common mode outputs always depend on the equivalent common mode excitation V_{in} instead of V_A, V_B and V_C separately, the model shown in the Fig. 9 can be further simplified to the bearing current model shown in Fig. 10.

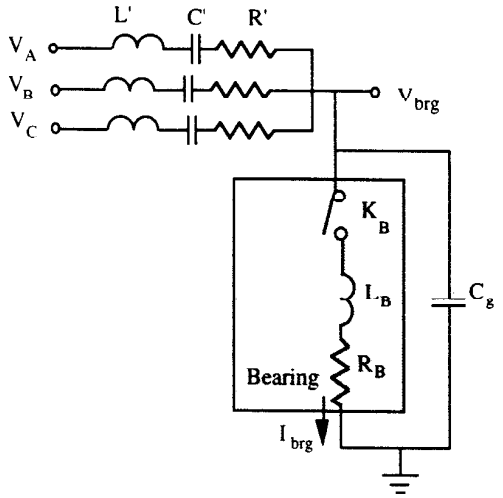

Fig. 9 Combination of Bearing Model to Rotor Coupling Circuit

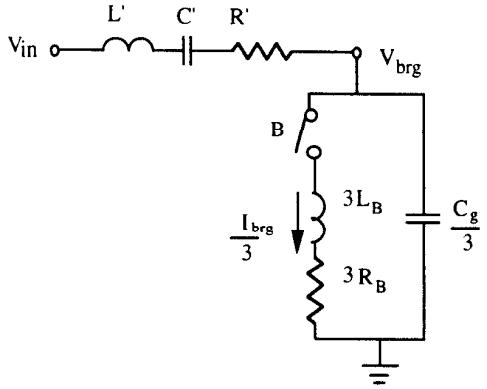

Fig. 10 Simplified Bearing Current Model

5. Simulation and Experimental Verification of the Models

With the above models, system identification procedures can now be initiated to determine all of the parameters of each model. Given an initial guess of parameters, the model shown in Fig. 6 and 10 are used to calculate the output variables. The results are then compared with experimental measurement until a set of optimal parameters is found. To avoid the uncertainty of dealing with the ground path impedance of the common mode, the motor case has been connected to the negative DC bus (as voltage reference) which forces the equivalent common mode voltage internal impedance to equal zero. In this configuration, an experimental measurement of a neutral point voltage and

grounding cable current (neglecting the contribution of bearing current) waveforms are shown in Fig. 11a). With the parameters listed in Table I, the calculation results based on the stator coupling model of Fig. 6 are plotted in Fig. 11b). By comparing Fig. 11a) and 11b), it is seen that the waveforms are almost identical. Therefore, it is apparent that the parameters can be identified satisfactorily in this manner.

Similar system identification procedures has been performed to determine the parameters of the bearing current model. The identification is based on the experimental measurement of responses of bearing voltages V_{brg} and currents I_{brg} to the common mode excitation. For a step input of common mode voltage V_{in}, a plot of the experimental measured bearing voltage V_{brg} is shown in Fig. 12a). As the bearing voltage is seen to charge up during each inverter switching, it is apparent that switch B in the bearing model must be open. Therefore, based on the waveforms and the corresponding circuit model, we can identify L′, C′, R′ and C_g. Fig. 12b) shows a simulated response based on the model of Fig. 9 and the identified parameters

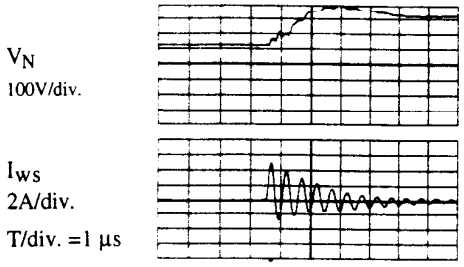

a) Measured response of V_N and I_{ws} to a step V_{in}

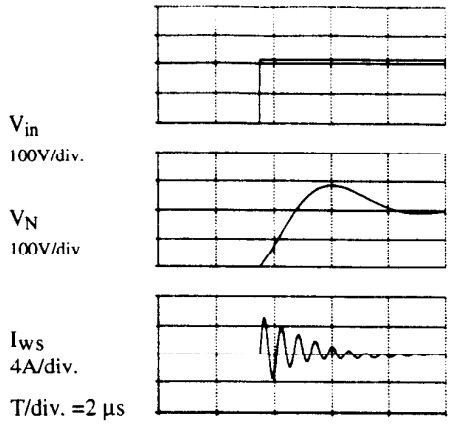

b) Calculated response of V_N and I_{ws} to a step V_{in}

Fig. 11 Comparison of Measured and Simulated Motor Neutral Voltage and Grounding Currents

Table I The Identified Parameters of Stator Coupling Model

L_O = 500 μH	C_O = 500 nF	R_O = 100 Ω
L_n = 10 nH	C_n = 5 nF	R_n = 100 Ω
L_l = 11 μH	C_l = 800 pF	R_l = 15 Ω

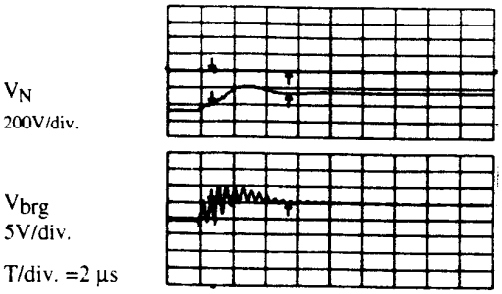

a) Measured neutral point and shaft voltage waveforms

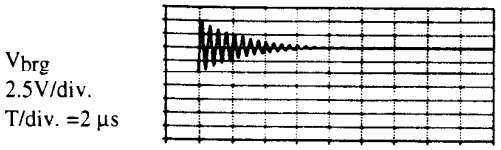

b) Simulated shaft voltages under same excitation condition

Fig. 12 Comparison of Measured and Simulated Bearing Voltages

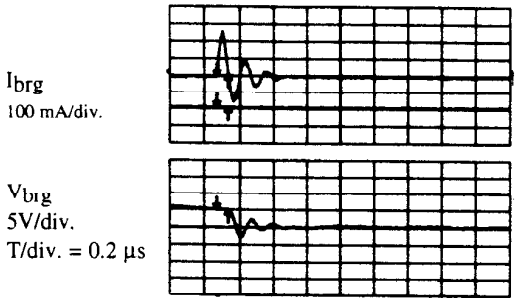

a) Measured bearing current spike and shaft voltage

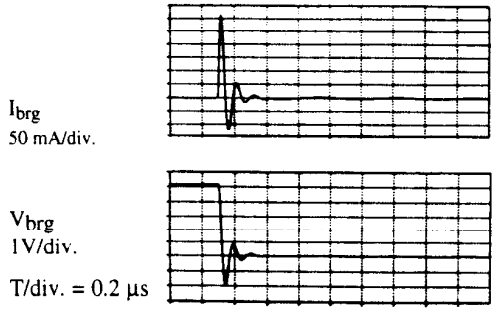

b) Calculated bearing current spike and shaft voltage

Fig. 13 Bearing Current Spike Caused by Discharge of Airgap Capacitor

Table II The Identified Parameters of Bearing Current Model

$L' = 300\ \mu H$	$C' = 20\ pF$	$R' = 200$ ohms
$L_B = 150\ nH$	$C_g = 800\ pF$	$R_B = 6.5$ ohms

listed in Table II. The identification of L_B and R_B are based on Fig. 13a) which shows a current spike produced by the discharge of the airgap capacitor C_g after switch B is closed.

Based on the identified parameters in Tables I and II, simulations have been performed to compare with numerous other experimental results. Fig. 14 shows one of the important results. In Fig. 14, the motor neutral point voltage is seen to increase step by step which corresponds to similar step-up in common mode voltage excitation V_{in} caused by PWM switching in the inverter. The bearing or shaft voltage V_{brg} follows the pattern of the motor neutral point voltage. This behavior is due to the capacitor divider effect of Cg and C_{WI}'s. The measured bearing current during the shaft voltage charge-up is seen to be almost zero due to high impedance inside the bearings. However, an abrupt voltage drop in bearing voltage accompanied by a large bearing current spike is observed which is actually caused by the sudden short circuit behavior inside the bearings. After bearings become short-circuited, some dv/dt related bearing currents begin to appear. By comparing the experimental measurement with the simulation traces in Fig. 14, it is seen that the results are almost identical except the difference in bearing voltage ringing during the transient which is believed to be caused by instrumentation error. Therefore, the bearing current and motor grounding currents model is clearly able to properly describe bearing current phenomena in inverter drives

6. Conclusions

This paper briefly discusses the mechanism of bearing current generated by PWM inverters which is related to the common mode voltages and parasitic capacitive couplings. Equivalent lumped parameter circuit models have been derived to describe the coupling from windings to stator and rotor respectively. Simulation is then performed to identify the model parameters by matching the simulated results with those of experimental measurement. The bearing currents model and stator coupling model is shown to be able to predict the motor bearing currents and the grounding currents. Comparison of the predicted results with realistic experimental measurements on a specially equipped motor shows good agreement. The bearing current model should prove useful for understanding of the phenomenon and for assisting in the determination of a feasible solution to the problem. The motor grounding current model can also be applied to the analysis of conducted EMI generation in motor-inverter systems.

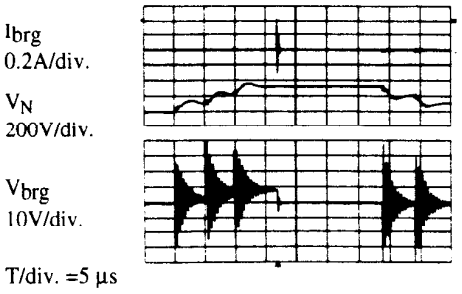

a) Experimental observation of bearing current generation

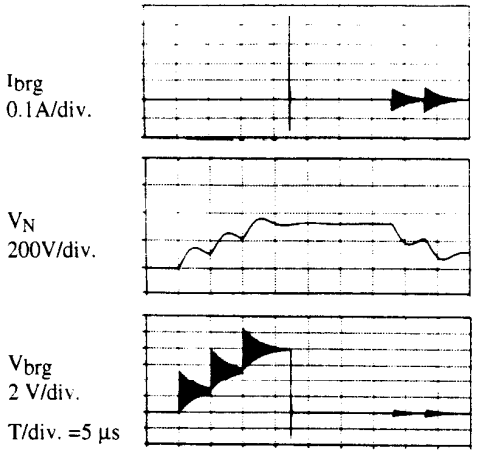

b) Simulation of bearing current generation

Fig. 14 Process of Bearing Current and Shaft Voltage Generation

References:

[1] S. Chen, T. A. Lipo and D. Fitzgerald, "Measurement and Analysis of Induction Motor Bearing Currents in PWM Inverter Drives", accepted for presentation at the International Aegean Conference on Electrical Machines and Power Electronics, Kusadasi, Turkey, June, 1995.

[2] S. Chen, T. A. Lipo and D. Fitzgerald, "Source of Induction Motor Bearing Currents Caused by PWM Inverters", to appear at Summer Meeting of IEEE Power Engineering Society, July, 1995.